Electrical Engineering (2019) 101:995–1006
https://doi.org/10.1007/s00202-019-00836-3

ORIGINAL PAPER

Multi-objective Pareto and GAs nonlinear optimization approach for flyback transformer

Sobhi Barg[1] · **Kent Bertilsson**[1]

Received: 16 February 2019 / Accepted: 11 September 2019 / Published online: 25 September 2019

Abstract
Design and optimization of high-frequency inductive components is a complex task because of the huge number of variables to manipulate, the strong interdependence and the interaction between variables, the nonlinear variation of some design variables as well as the problem nonlinearity. This paper proposes a multi-objective design methodology of a 200-W flyback transformer in continuous conduction mode using genetic algorithms and Pareto optimality concept. The objective is to minimize loss, volume and cost of the transformer. Design variables such as the duty cycle, the winding configuration and the core shape, which have great effects on the former objectives but were neglected in previous works, are considered in this paper. The optimization is performed in discrete research space at different switching frequencies. In total, 24 magnetic materials, 6 core shapes and 2 winding configurations are considered in the database. Accurate volume and cost models are also developed to deal with the optimization in the discrete research space. The bi-objective (loss–volume) and tri-objective (loss–volume–cost) optimization results are presented, and the variations of the design variables are analyzed for the case of 60 kHz. An example of a design (30 kHz) is experimentally verified. The registered efficiency is 88% at full load.

Keywords Genetic algorithms · NSGAII · Pareto front · Flyback converter · Transformer · Core loss · Winding loss

List of symbols

V_{in}, V_{out}, P_{in}, P_{out}	Input and output voltage and power
P_t, P_c, P_w	Transformer, core and winding losses
D, l_g, J	Duty cycle, air gap, current density
V_p, V_s, I_p, I_s	Primary and secondary voltage and current
N_{lp}, N_{ls}, N_{tp}, N_{ts}	Primary and secondary number of layers and number of turns per layer
C_c, W_c	Core cost and winding configuration
d_p, d_s	Primary and secondary diameters
l_c, l_m	Mean core length and mean turn length
I_{pmax}, I_{smax}	Primary and secondary maximum currents
I_{pavg}, I_{savg}	Primary and secondary average currents
I_{pr}, I_{sr}	Primary and secondary currents ripple
R_{dcp}, R_{dcs}	Primary and secondary DC resistance
F_r, Ac	Ac-to-dc resistance ratio, core section
x	Diameter-to-skin depth ratio
L_p, L_s	Primary and secondary inductance
B_{ac}, B_{max}	Swing and maximum flux density
N_p, N_s	Primary and secondary number of turns
V_{tr}, V_c, V_w	Transformer, core and winding volumes
μ_0, μ_r	Vacuum and relative permeability
I_{prms}, I_{srms}	Primary and secondary RMS currents
f, f_u	Frequency and winding filling factor

1 Introduction

Flyback converter is widely used in low-power applications such as laptop and mobile chargers. It has several advantages compared to other topologies, especially for low-power applications. On the other side, this topology presents one major inconvenient which is its limited power capability. The converter is only suitable for low power (< 150 W), and its efficiency degrades as the power increases. This is due to the conflict in the inductance design requirements. From one side, the inductance needs to be increased in order to allow more power storage capability during the on-time, and from the other side, it needs to be decreased because it is inversely

✉ Sobhi Barg
Sobhi.Barg@miun.se

[1] Mid Sweden University, Sundsvall, Sweden

proportional to the output power [1–6]. Several parameters and interdependent variables contribute in the design of the flyback transformer. The conflict in the design of the transformer inductance makes the optimization process a complex task which needs advanced design and optimization techniques to improve its performance.

Classical design techniques of inductive components are mainly the area product method and the core geometry coefficient [6, 7]. Both design approaches do not consider the nonlinearity of the design variables or/and the nonlinearity of the complete problem. Moreover, the variables are very dependent on each other which make the problem impossible to be solved accurately using these methods. Some other techniques were presented to optimize the magnetic devices by determining the optimum magnetic flux density; however, they do not solve the nonlinearity issue [8–10]. The limitations of these methods are discussed more deeply in Sect. 2.1.

The consideration of more than one objective in the optimization transforms the problem to a multi-objective problem which cannot be solved by the previous presented techniques. Some methods like the weighted sum method and the Min/Max method were used for this kind of problems [11]. However, they can only deal with convex and continuous functions which is not the case of the inductive components design problem.

Genetic algorithms and Pareto optimality concept starts to be a common solution in the design of electromagnetic devices in the last decade [11–22]. The main feature of the GAs is their capability to handle numerous optimization variables and objective functions without losing accuracy in the convergence to the optimum Pareto front. They are also very effective in solving problems with discontinuous variables, concave and convex, linear and nonlinear, constrained and non-constrained objective functions. Additionally, GAs allow also reducing the design time and eventually the cost. All the previous advantages make of the GAs a good candidate for the multi-objective optimization of the inductive components.

From another side, the convergence to the optimum set of solutions doesn't only depend on the performance of the optimization algorithms but more importantly on the problem formulation. This later includes the selection of the design variables, the design equations, the design constraints and the sequences between them. As an example, in some types of nonlinear problems, one variable or more can be at the same time an objective function and a design variable or it can also be a constraint. Few works were achieved to optimize the inductive components for power electronics such as [13] and [14]; however, no one of them addressed these issues. The goal of this paper is to deal with this problem. Particularly in this work, some crucial variables such as the duty cycle, which has a great effect on the transformer loss, the efficiency, the magnetic material and the winding configurations, are considered as main design variables. Finally, to improve the design objectives, reliable and accurate models of the objective functions, the design constraints and the intermediate design functions, such as core loss, winding loss and leakage inductance, are developed.

1.1 Research contributions

The main contributions of this work are:

1. To develop a multi-objective optimization approach to design a flyback transformer in continuous conduction mode using GAs and Pareto optimality concept.
2. To solve the nonlinearity of the design problem resulting from the interdependence between the design variables, the objective functions and the design constraints.
3. To include the effect of some crucial variables in the optimization process such as the duty cycle and the efficiency which are neglected in the previous works.
4. To analyze the variation of the design and optimization variables with respect to the Pareto front for the bi-objective (loss–volume) optimization and tri-objective (loss–volume–cost) optimization problems in order to get a clear picture on the variation of these variables with respect to the objective functions.
5. To verify the optimization results of the transformer designed for 30 kHz by experiments and comparison with existing approaches.
6. To give an insightful picture on the state-of-the-art on the design and optimization of inductive components.

This paper is organized as follows. A review of the optimization and design methods of inductive components is presented in the second section. The third section details the multi-objective design and optimization approach. The optimization results are highlighted and analyzed in the fourth section. The experimental verification and comparison with classical methods of a design case are shown in the fifth section. Finally, the advantages of the future works of the proposed design are summarized in the conclusion.

2 Review of the high-frequency inductive components design and optimization methods

2.1 Challenges in the design of HF transformer

The major challenges faced today by designers of high-frequency transformers are the selection of: the appropriate magnetic material, the suitable core shape, the required core size and the winding configuration. All the former variables

are generally chosen based on the designer experience to satisfy the design constraints and requirements which can reduce the design efficiency. The selection of the switching frequency and the duty cycle is defined arbitrarily. However, it was shown in the literature that the duty cycle presents a great effect on the core loss and the winding loss [22–32]. The frequency has also an important role in the transformer loss and volume. Thus, the consideration of these variables as main design and optimization variables is crucial. The determination of the number of turns, the calculation of the air gap and some other intermediate functions is derived from the relationships between the inductance reluctance model, the energy storage equation and Faraday's and Ampere's laws. These variables have nonlinear relationships between each other. Furthermore, the design of high-frequency transformers needs to take into consideration some constraints such as the leakage inductance and the temperature rise. In general, there is a huge interdependence and interaction between the design variables, the intermediate design functions, the design constraints and the objective functions which makes the problem very complex to be solved.

In a given design problem, one combination or more of the previous discussed design variables can be the optimum set of solutions for the objective functions such as the efficiency, the cost and the volume. In the following, the existing methods are analyzed and their limitations to solve the former issues are figured out. The existing methods can be classified into two categories: single-objective methods and multi-objective methods.

2.2 Single-objective methods

The area product method was early developed to select the suitable magnetic core for a given application [6, 7, 33]. It is a geometry dimensional factor of magnetic cores which has an equivalent term of electrical variables of the power converter. The equivalent term depends on the maximum magnetic flux density. The geometry term is the product of the core window area and the core cross section. In the literature, there are several forms of the area product. Some correction factors are adopted by industrials in order to meet the design requirements [34–36]. For example, author in [34, 35] has proposed that the volume of the flyback transformer is twice the one for forward. This correction factor is used because the flyback transformer needs to store energy during the on-time. In [2], a monogram of the area product as a function of the stored energy is given in [36], and the area product was expressed as a function of the magnetizing inductance to take into consideration the effect of the DC current and the stored energy.

The first drawback of the area product (AP) method is that it includes the filling factor which is an unknown and usually estimated to 0.3 or 0.4. Secondly, the product between the core section and the window area doesn't give a real picture and an accurate characterization of the core shape. In other terms, the area product does not take into account the core shape effect on the design because two different core shapes can have the same AP. Furthermore, the area product method allows only getting an idea about the required core size; however, all the remaining variables, such as the material and the winding configuration, are chosen by the designer using his own experience. In addition to that, this method does not minimize the transformer loss because it doesn't include the eddy currents effect at high frequency.

The core geometry coefficient method is also a geometry dimensional factor. The expression of the core geometry coefficient is derived from the formula of the optimum magnetic flux density that yields to minimum transformer/inductance loss. It includes the core length in addition to the core window and the core cross section which can improve the accuracy in the selection of the suitable magnetic core. It also includes the Steinmetz parameters, characterizing the core loss of the magnetic materials. This feature offers the possibility to consider the effect of the magnetic material loss in the design process, and therefore the selection of the best material becomes achievable [37].

Although the core geometry coefficient offers better accuracy in the selection of the suitable magnetic core than the area product, it still presents major limitations which are summarized as follows: (1) the method is a single-objective design approach used to improve the efficiency and not the cost or the volume, (2) the method is only suitable at fixed frequency and fixed duty cycle, and (3) the method needs an iterative approach to include the effect of the core shape because magnetic core with different shapes might have the same core geometry.

Hurley developed an improved expression of the equivalent term of the area product to include high-frequency effects such as the skin and the proximity effects as well as the temperature effect. This was achieved by calculating the optimum magnetic flux density instead of using the maximum magnetic flux density [9, 10].

A similar approach based on the determination of the optimum magnetic flux density was presented by Petkov but without consideration of the high-frequency effects [8].

In [38], the weighted efficiency method was applied to optimize the flyback inverter, including the transformer component, for photovoltaic applications. The optimization of the weighted function was solved by the differential evolution method.

2.3 Multi-objective methods

In the former design approaches, the efficiency is the only objective to deal with as it is the major concern of

the designer. In the last decade, designers are much more interested to optimize, not only the converter efficiency, but also the cost and the volume in order to meet the standards and clients requirements. This is called a multi-objective optimization problem. Genetic algorithms are powerful optimization methods to solve this kind of problems. Pareto front is also one insightful and effective tool to represent the optimum solution in the objectives space or variables space. Using Pareto optimality concept, the decision maker can move along the Pareto front to select one of the optimal solutions that meets the required needs. It is also possible to know the evolution of the optimization variables and any intermediate function with respect to Pareto front. Hence, the effect of every variable can be well understood and analyzed. In fact, using GAs and Pareto concept of optimality, we can get a clear picture of the full problem in the objective space and the intrinsic variation of the design variables can be seen at any optimal operating point [11, 19–21]. In [12], GAs was used to achieve the best tradeoff between volume and loss of PWM inverter output filters. In [13], the loss and weight optimization of medium frequency transformers was performed using genetic algorithms (NSGAII). The main limitation of this work is that the capability of the GAs to solve nonlinear problems is not fully utilized. As an example, in [13], the value of the required inductance was initialized in the design of LLC and DAB converter. GAs was applied to determine the optimum set of the variables given by the inductance reluctance model independently of the converter operation constraints. However, to be more accurate, the value of the required inductance depends on several other variables, depending on the converter topology, such as the duty cycle, the frequency and the efficiency. In a similar way in [14], the magnetizing inductance was considered as a fixed parameter for LLC converter which is not enough accurate design approach.

Generally speaking, in the previous discussed works, the dependency of required inductance on the converter requirements (efficiency, duty cycle, frequency, etc.) was neglected and this can reduce the design accuracy. Another important issue which was not clearly explained and formulated in previous work is the relationship between the different optimization variables, the objective functions and the design constraints which all contribute in the nonlinearity of the design problem. Additionally, the models of the objective functions present lack of accuracy such as the negligence of the temperature effect on the core loss.

In [15], two kinds of evolutionary algorithms (GA and PSO) have been tested to optimize the volume and the mass of EI and UI core inductor, respectively. A continuation of the work presented in [15] is exhibited in [16]. The single optimization (volume) and the bi-objective optimization (loss vs. volume and loss vs. cost) of the EI inductor are performed. The tri-objective optimization is also presented by optimizing the cost and the volume constrained to the objective function loss. The single-objective optimization is presented with continuous and discrete variables. GOSET optimization tool, developed by authors in [17, 18], was used to achieve the optimization process. It was shown that GOSET tool allows achieving better minimization with discrete variables. The structure of GOSET is similar to NSGAII but with more optional function that improves its performance. In [19], a multi-objective optimization approach was presented to minimize the losses, the weight and the volume of power inductors for three-phase high power density inverter.

2.4 200-W flyback converter design complexity

Designing a 200-W flyback converter is very complicated due to the reasons discussed previously. In the literature, there are few attempts done to realize a flyback converter at this power level. The only industrial 200-W flyback converter was designed by Texas Instruments. The adopted solution consists in using two interleaved transformers with an inductance of 500 µH each, and the switching frequency is 100 kHz. The value of the inductance reflects the significant volume of the used transformers [39]. Another company developed a 140-W flyback converter, but it can supply a maximum power of 200 W [40]. The inductance of the transformer is 300 µH. Another study in [41] showed the design of a 180-W flyback converter using a regenerative snubber circuit concept. The magnetizing inductance is 102 µH, and the switching frequency is 80 kHz.

In all the previous designs, the use of a big inductance is necessary to reach the 200-W output. In the following, GAs and Pareto front optimality concept is used to optimize the 200-W flyback transformer.

3 Design approach

3.1 Problem description

The objective is to perform the bi-objective (loss–volume) and tri-objective (loss–volume–cost) optimization of high-frequency transformer for a 200-W flyback converter. The characteristics of the converter are summarized in Table 1.

Table 1 Converter characteristics

Output voltage	120 V
Input voltage	48 V
Output power	200 W
Maximum temperature rise	60 °C
Frequency	10–20–30–40–50–60 kHz

Several variables and constraints contribute in the design of flyback transformer. As per our knowledge, still there is no study solving the optimization of this magnetic problem with consideration of all variables due to the issues discussed in Sect. 2. Using the advantages of GAs, the optimization of the flyback transformer with consideration of all the design variables becomes possible. All the data of the magnetic cores and magnetic materials are summarized in Tables 5, 6 and 7.

3.2 Core loss prediction

Several empirical models have been developed to calculate magnetic core loss of high-frequency inductive components used in switching power supplies. These models, which are the modified Steinmetz equation, the generalized Steinmetz equation (GSE), the improved GSE and the improved^2 GSE, are derived from the Steinmetz equation [23–27]. They present some limitations which are explained in [22]. The model given in [22] [Eq. (1)] solves the limitations of the former models. Its main features are: high accuracy especially at low duty cycle, compact, reliable and easy to apply.

$$\langle P_c \rangle = \frac{\pi}{4}\left[\begin{array}{l} k_1 D\left(\frac{f}{2D}\right)^{\alpha_1}\left(B_{ac}\right)^{\beta_1} \\ \quad +k_2(1-D)\left(\frac{f}{2(1-D)}\right)^{\alpha_2}\left(B_{ac}\right)^{\beta_2} \end{array}\right] V_c \tag{1}$$

In this work, the Steinmetz parameters are expressed as a function of the frequency in order to improve the reliability of the optimization algorithm [22]. Figure 1 shows how accurately the Steinmetz parameters are derived and the high consistency between the manufacturer data and the developed model for material N27.

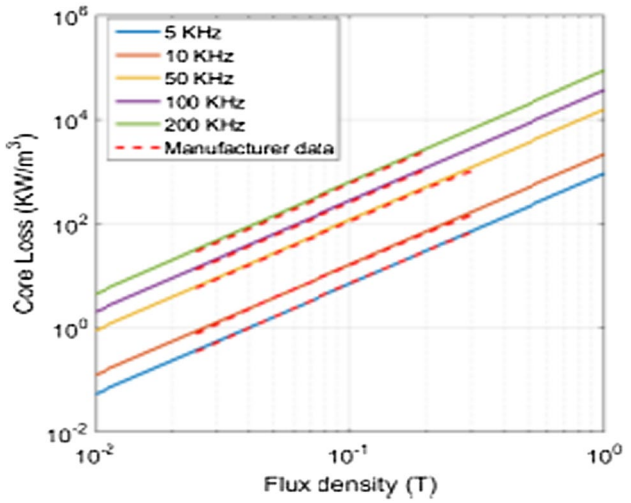

Fig. 1 Modeling of core loss curves for N27

To include the effect of the temperature, the following equation was developed using curve fitting technique of the core loss given in manufacturer's catalogs. It is multiplied to Eq. (1):

$$f(T) = a_0 T^2 + a_1 T + a_2 \tag{2}$$

3.3 Winding loss

At high frequency, the skin effect and the proximity effect are significant and their impact on the AC resistance is very huge. In the literature, there are various models to account the effect of these phenomena such as Dowel's formula and Ferreira's formula [28, 29]. Dowell's formula has shown a good accuracy and consistency with measurements [30–32]. For this reason, it is applied in our design. The winding loss can be expressed as follows:

$$P_w = R_{dcp} F_{rp} I^2_{prms} + R_{dcs} F_{rs} I^2_{srms} \tag{3}$$

$$F_r = x\left[\frac{e^{2x} - e^{-2x} + 2\sin 2x}{e^{2x} - e^{-2x} - 2\cos 2x} + \frac{2\left(N^2-1\right)}{3}\frac{e^{2x} - e^{-2x} - 2\sin 2x}{e^{2x} - e^{-2x} + 2\cos 2x}\right] \tag{4}$$

3.4 Volume modeling

The volume models presented in the literature are not enough accurate and cannot be applied for all geometries. The winding configuration and the core reference are two optimization variables as it is given in Sect. 3.6. For that reason, a volume model was developed for each configuration and each core geometry. In the following, we detail the volume model using EE core with split winding (see Fig. 2). The objective is that the developed model should be expressed as a function of the optimization variables to improve the algorithm reliability.

$$V_c = L_c A_c \tag{5}$$

$$A_c = DF \tag{6}$$

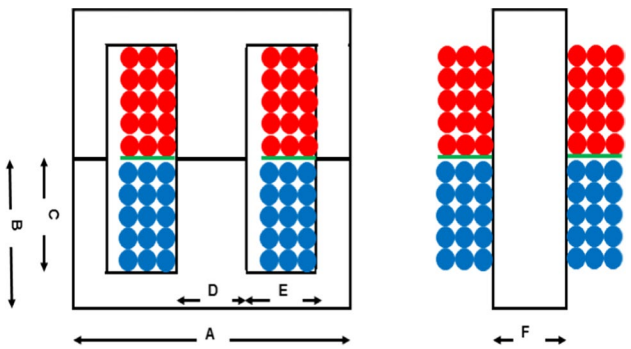

Fig. 2 Core type EE with split winding configuration

The primary winding volume is equal to:

$$V_{wp} = 2N_{tp}d_p^2\left(F + D + 2N_{lp}d_p\right) \tag{7}$$

Similarly, the secondary winding is calculated.

3.5 Transformer cost modeling

The cost model is derived using curve fitting technique from the data in [39, 42]. It is a function of the volume, the magnetic material and the geometry.

$$C_c = k\left(aV_c^b + c\right) \tag{8}$$

Parameter k represents the geometry cost effect, and a, b and c are parameters depending on the magnetic material.

3.6 Problem formulation

The objective of this work is to minimize the loss, the volume and the cost of the flyback transformer. Their models are given in the previous subsections. In order to achieve an accurate design, a good understanding of the design equations as well as the dependency and interaction between the optimization variables, the design constraints and objective functions is mandatory.

The full design equations of the flyback converter are given in Eqs. (9–13). As it can be seen in Eq. (10), the efficiency is a design variable. Simultaneously, it represents the first objective function as it reflects the total loss. This later appears also in Eq. (19) as a design constraint of the temperature rise. This clearly represents one aspect of nonlinear problem. In order to deal with this issue, an optimization variable referred to as "effective efficiency" is generated as shown in Table 2. Then, by imposing an equality constraint between the efficiency (objective function) and the effective efficiency (variable), the problem can be solved. The same idea is performed for the air gap which has an effect on the inductance and the core saturation as given in Eqs. (9 and 16).

GOSET optimization tool, discussed in Sect. 2.3, is used in our work. The optimization flowchart is given in Fig. 3. For one iteration, a set of variables, given in Table 2, is randomly chosen by the algorithm and applied for the different calculation steps. The calculation phase includes the design equations, the design constraint, the objective functions and the intermediate functions. Solutions which do not satisfy the design constraints are discarded; however, those which fulfill the requirements are ranked to form the Pareto front of the *i*th iteration. The process is repeated until the Pareto front is reached. The needed number of iteration is defined by the user.

Table 2 Design space for the discrete research spaces

Variable	Unit	Type	Interval
Magnetic material	U	Integer	[1–24]
Duty cycle	–	Integer	[1–72]
Core reference	U	Integer	[1–*n*]
W_c	U	Integer	[1–2]
N_p	U	Integer	[1–100]
N_s	U	Integer	[1–100]
d_p	U	Integer	[1–60]
d_s	U	Integer	[1–60]
l_g	M	Real	[1e−4, 4e−3]
η_i	–	Real	[0.95–0.99]

3.6.1 Design equations of the transformer

The design equations of the flyback transformer are summarized below.

$$L_p = \frac{\mu_0\mu_r N_p^2 A_c}{\left(l_c + l_g\mu_r\right)}; \tag{9a}$$

$$L_s = \frac{\mu_0\mu_r N_s^2 A_c}{\left(l_c + l_g\mu_r\right)} \tag{9b}$$

$$P_{in} = \frac{P_{out}}{\eta_i} \tag{10}$$

$$\begin{aligned} I_s &= \frac{P_{out}}{V_{out}}; \quad I_{savg} = \frac{I_s}{(1-D)}; \quad I_{srms} = \frac{I_s}{\sqrt{(1-D)}} \\ I_{sr} &= \frac{V_{out}(1-D)}{L_s f}; \quad I_{smax} = \frac{I_{sr}}{2} + I_{savg} \end{aligned} \tag{11}$$

$$I_p = \frac{P_{in}}{V_{in}}; \tag{12a}$$

$$I_{pavg} = \frac{I_p}{D}; \tag{12b}$$

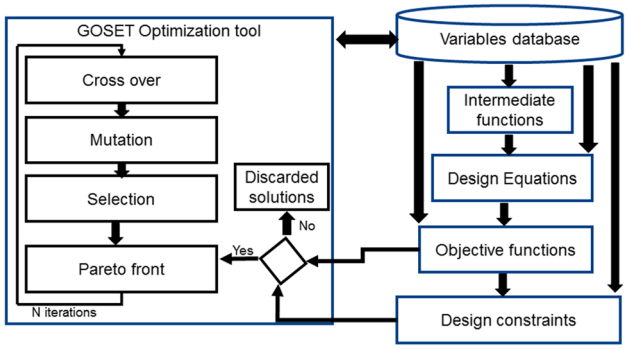

Fig. 3 Flowchart of the optimization tool

$$I_{\mathrm{pr}} = \frac{V_{\mathrm{in}} D}{L_{\mathrm{p}} f} \tag{12c}$$

$$I_{\mathrm{prms}} = \frac{I_{\mathrm{p}}}{\sqrt{D}}; \tag{12d}$$

$$I_{\mathrm{pmax}} = \frac{I_{\mathrm{pr}}}{2} + I_{\mathrm{pavg}} \tag{12e}$$

$$B_{\mathrm{ac}} = \frac{V_{\mathrm{in}} D}{f N_{\mathrm{p}} A_{\mathrm{c}}}; \tag{13a}$$

$$B_{\mathrm{max}} = \frac{B_{\mathrm{ac}} I_{\mathrm{pmax}}}{I_{\mathrm{pr}}} \tag{13b}$$

3.6.2 Design constraints

The design constraints are summarized as follows:

- The core saturation, the gain and the air gap are as follows:

$$B_{\mathrm{max}} \leq 0.7 B_{\mathrm{s}} \tag{14}$$

$$\mathrm{Gain} = \frac{N_{\mathrm{s}} D}{N_{\mathrm{p}}(1 - D)} \tag{15}$$

$$l_{\mathrm{g}} = \frac{\mu_0 I_{\mathrm{pmax}}^2 L_{\mathrm{p}}}{A_{\mathrm{s}} B_{\mathrm{max}}^2} - \frac{l_{\mathrm{c}}}{\mu_{\mathrm{r}}} \tag{16}$$

- Conductor diameters: They are determined by [31].

$$d_{\mathrm{p}} = \sqrt{\frac{I_{\mathrm{pmax}}}{7.2}}; \quad d_{\mathrm{s}} = \sqrt{\frac{I_{\mathrm{smax}}}{7.2}} \tag{17}$$

- The winding area A_{w} should be capable of allocating the two windings. f_{u} is equal to 0.4.

$$A_{\mathrm{w}} \geq \frac{\pi\left(N_{\mathrm{p}} d_{\mathrm{p}}^2 + N_{\mathrm{s}} d_{\mathrm{s}}^2\right)}{f_{\mathrm{u}}} \tag{18}$$

- Temperature rise T_{r}:

$$T_{\mathrm{r}} = \frac{53\left(P_{\mathrm{c}} + P_{\mathrm{w}}\right)}{V_{\mathrm{c}}^{0.53}} \leq 60\,^{\circ}\mathrm{C} \tag{19}$$

- Currents ripple factor: it should be lower than r_{max}.

$$I_{\mathrm{pr}} \leq r_{\mathrm{max}}; \quad I_{\mathrm{sr}} \leq r_{\mathrm{max}} I_{\mathrm{savg}} \tag{20}$$

- Peak MOSFET voltage: the maximum allowable voltage across the MOSFET time must be lower than 400 V.
- Leakage inductance: it is kept lower than 2% of the magnetizing inductance. Model presented in [42] is used.

3.6.3 Optimization variables

The optimization variables are highlighted in Table 2. They are of two types: integer and real.

4 Multi-objective optimization in discrete research space

4.1 Bi-objective optimization

The results of the GA-based optimization for different frequencies are shown in Fig. 4. The first important thing that can be noticed is the intersection of the Pareto fronts between each other which shows that the dominance of each one depends on the design region in the volume–loss plan. Using Pareto front, the designer has the ability to select the best switching frequency depending on the requirements in term of loss and volume. Generally, 60 kHz can be considered as the optimum frequency. The second optimum frequency is 50 kHz. In the volume region [50–600] cm^3, the dominant Pareto front is in the descendant frequency order except around 200 cm^3 where 30 kHz dominates 40 kHz. The minimum optimum volume that can be achieved is 21 cm^3 realized with 60 kHz. This volume yields to a total loss of 5.9 W. The minimum total loss is 1.8 W achievable either with 500 cm^3 and 50 kHz or with lower volume and 60 kHz.

The best magnetic material that offers minimum loss and minimum volume is F of type ferrite manufactured by

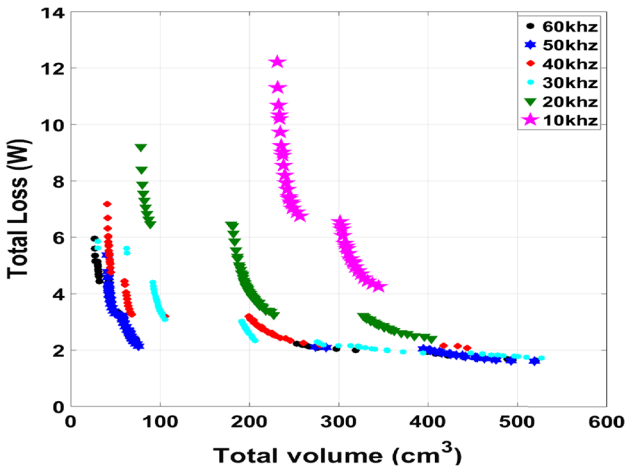

Fig. 4 Pareto fronts of loss versus volume

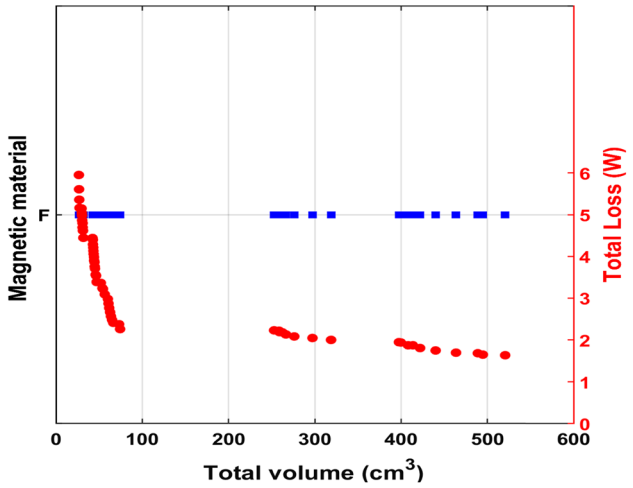

Fig. 5 Magnetic material versus Pareto front

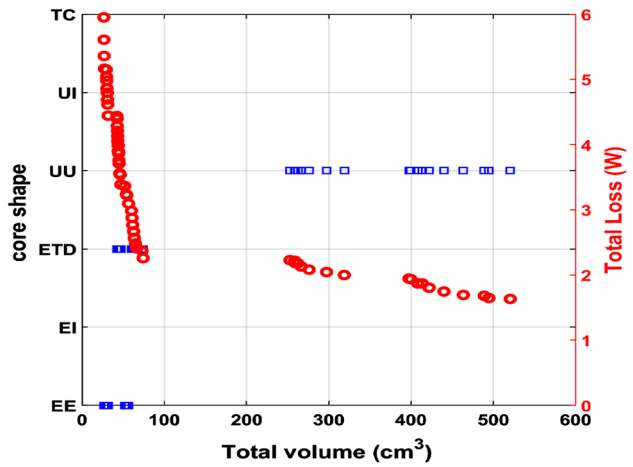

Fig. 6 Core shape versus Pareto front (see Table 7)

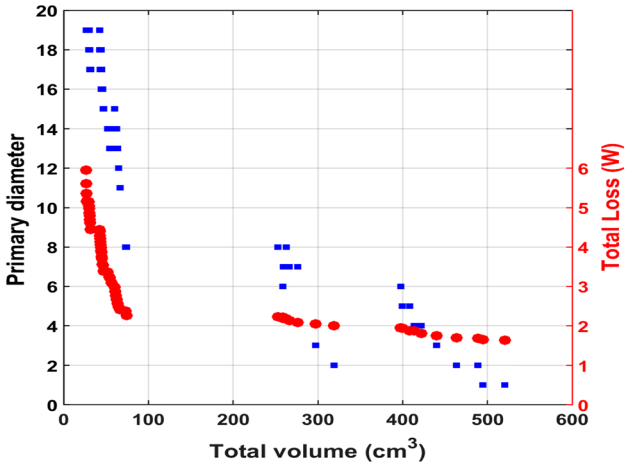

Fig. 7 Primary diameter versus Pareto front

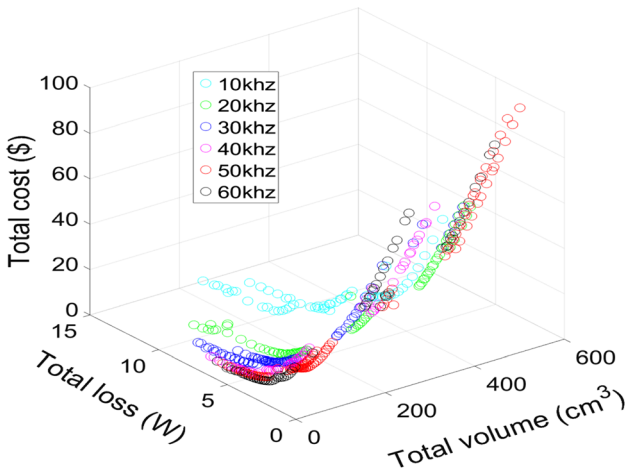

Fig. 8 3D Pareto front of loss–volume and cost

Magnetics (Fig. 5). This material has the second highest permeability (3000) among all the ferrite materials in the database, which helps to reduce the magnetizing current and therefore minimize the core loss. It has also the second least specific core loss among all ferrite materials at 60 kHz.

EE and ETD shapes are the best geometries for small volume (< 100 cm^3) and UU and Toroid for big volume (Fig. 6). The choice of UU and Toroid shape for big volume is not because of their performances but because they are the only shapes available with this volume (Table 7).

The diameter of the primary winding increases with the increase in the transformer volume and the decrease in the total loss (Fig. 7).

The results of the tri-objective optimization are depicted in Fig. 8. It can be seen that the 60 kHz keeps almost the best solution. A better way to see the distribution of the Pareto set is to use a 2D plan for two objective functions, and the third one can be read using color bar tool as given in Fig. 9 for the case of 60 kHz. The loss decreases with respect to volume; however, the cost is not (Fig. 10).

Using the normalized Euclidean distance to ideal solution (Eq. 21), the best optimum solution can be determined for the different cases. Their details are shown in Table 3

$$d_{\text{is}} = \sqrt{\sum_{i=1}^{n} \left(\frac{f_i(x) - f_i^{\min}}{f_i^{\min}} \right)^2} \tag{21}$$

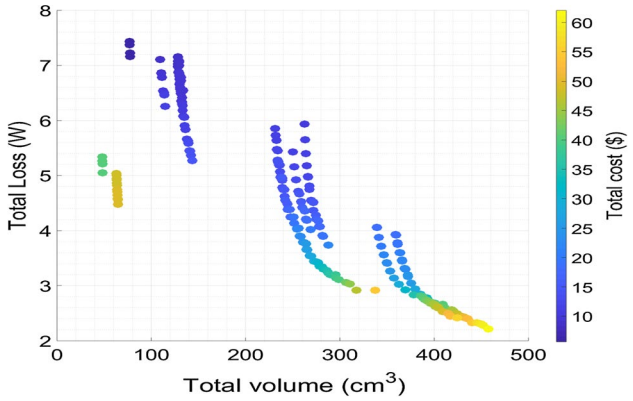

Fig. 9 Pareto front loss–volume–cost for the case of 60 kHz

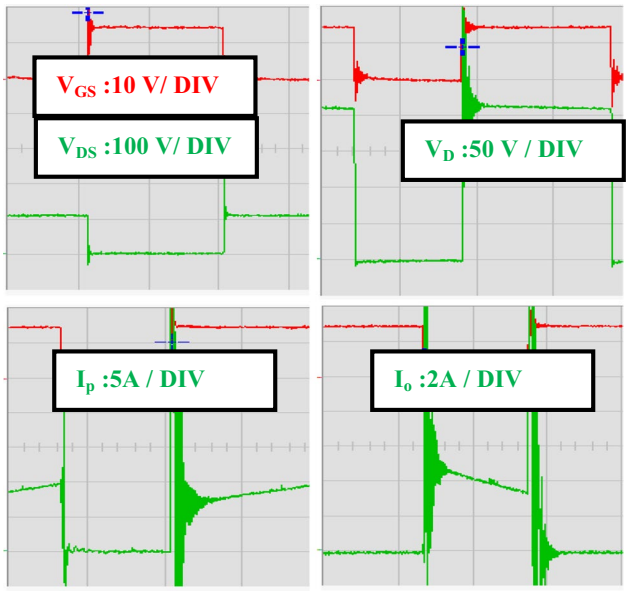

Fig. 10 Experimental flyback converter waveforms at 30 kHz (time division is 6.66 µs/div)

Table 3 Details of the design solutions

	30 kHz	40 kHz	50 kHz	60 kHz
Losses (W)	4.88	4.37	4.02	3.66
Cost ($)	5.68	3.9764	3.96	3.32
Volume (cm^3)	63.41	44.11	44.12	42.75
Material/W_c	F/2	F/2	F/2	F/2
Shape/Ref	ETD/7	ETD/6	ETD/6	ETD/6
d_p (mm)	1.82	1.8	1.82	2.05
d_s (mm)	0.91	1.02	1.02	0.91
N_p/N_s	23/47	24/27	17/32	9/37
l_g (mm)	1	0.7	0.6	0.5

5 Comparison with classical area product method and experimental verification

The optimum magnetic material that is selected by the optimization algorithm is F material provided by Magnetics. But, at the time of the experimental implementation, this selected core was not available in the market. For that reason, the optimization process was run a second time and the results show that R material is the new optimum one. No changes were registered for other variables (core reference, number of turns, duty cycle, etc.).

5.1 Comparison with the area product methods

The objective of this section is to compare the outputs of the design case 30 kHz with the outputs of two single-objective design approaches in order to verify the reliability and the accuracy of our results and to get an approximated idea about the efficiency of the design.

The two classical design techniques are the approach of Lloyd from Texas Instruments and the Approach of Sanjaya [34–36]. To give a fair comparison between the different approaches, we have used the same magnetic material which is the optimal one selected by the proposed approach (ferrite F). The duty cycle was fixed to 0.5 for the classical techniques. For the brevity of the paper, we highlight the most important steps of the design in Table 4.

It is clear from Table 4 that the proposed approach yields to better theoretical efficiency than other design techniques. However, Sanjaya approach leads to the worst efficiency resulting from the high number of winding layers. The second approach of Lloyd allows getting the same magnetic core as the one selected by the proposed approach; however, the transformer loss is bigger because of the reduced size of the winding conductors. The first approach of Lloyd has comparable efficiency to our design but with bigger magnetic core.

In comparison with the design solutions given in Sect. 2.3, the inductance of the designed transformer is 233 µH at 30 kHz which is much lower than the one designed by Texas and the one proposed by ON Semiconductor.

5.2 Experimental results

An IGBT STGFW30V60F is used, and it is controlled using a driver TC4429. A capacitor of 63 V 2200uF is used in the input, and a 400 V 47 µF for the output filter. The rectifier diode is Mur1560. The sensing resistors in the input and output are 0.1 Ω, 5 W.

The obtained waveforms of the input and output currents, the IGBT voltage and the diode voltage are shown in Fig. 8.

Table 4 Comparison of the design outputs between the proposed approach and the classical techniques (30 kHz design case)

	Proposed approach	Lloyd approaches [36]		Sanjaya approach [34]
		1st approach	2nd approach	
Primary inductance (μH)	233	216.45		216.45
Maximum swing flux (T)	0.1	0.1		0.1
Area product (cm^4)	–	17.78	10.24	2.09
Selected core	ETD59	EE 65	ETD59	ETD49
Selected material	F	F		F
Turns ratio	0.48	0.4		0.4
Primary/secondary number of turns	23/47	15/38	22/55	38/95
Primary/secondary diameter (mm)	1.82/1.45	1.28/0.77		1.28/0.77
Primary/secondary number of layers	1/1	1/1		2/2
Primary/secondary resistance (mΩ)	81.12/327.52	76.54/396	112.25/574	663/2100
Winding loss (W)	4.72	5.44	7.94	39
Core loss (W)	0.17	0.27	0.17	0.08
Transformer loss (W)	4.88	5.71	8.11	39.08

The efficiency reaches up to 88% at full load. This efficiency is very acceptable for a 200-W flyback converter operating at 30 kHz. The obtained results can be improved by better selection of the switching devices. However, we are limited to use only devices available in the laboratory because it is not the objective of this work to optimize the full converter.

6 Conclusion

The paper proposes a multi-objective optimization approach of flyback transformers in discrete research space using GAs. The key conclusions of this paper are summarized as follows:

- The approach solves the limitations of the existing works by considering the effect of the duty cycle and the efficiency as main optimization variables. The approach takes also into account the nonlinear relationships between variables, objective functions and design constraints.
- The proposed approach allows better minimization of the loss and volume in comparison with existing classical methods.
- The approach is very effective as it improves the accuracy of the results compared to other techniques, and it reduces the design time. The optimization needs 30 min to get the optimum Pareto fronts which can take longer time using classical techniques.
- Results show that the optimal magnetic material and optimal core shape depend on the switching frequency.
- Pareto fronts of the objective functions (loss, cost and volume) are inversely proportional to the switching frequency.

Acknowledgements Open access funding provided by Mid Sweden University.

Appendix

See Tables 5, 6 and 7.

Table 5 Magnetic material characteristics [43–47]

Material	Type	Provider	Permeability	B_s	T_c (°C)
N27	Ferrite	EPCOS	2000	0.5	220
N87		EPCOS	2200	0.49	210
R		Magnetics	2300	0.47	210
P			2500	0.47	210
F			3000	0.47	210
M75		Ferroxcube	5000	0.43	140
A1	Tape wound core (nickel iron alloy) similar to amorphous	Magnetics	40,000	1.58	500
D1			100,000	0.82	460
F1			40,000	0.82	460
A2			40,000	1.58	500
D2			100,000	0.82	460
F2			40,000	0.82	460
H2			50,000	1.4	500
F3M	Crystalline	Hitachi	40,000	1.23	570
Kool mu 26u	Powder	Magnetics	26	1	500
Kool mu 40u			40	1	500
Kool mu 60u			60	1	500
Kool mu 90u			90	1	500
Kool mu 125u			125	1	500
MPP 14u			14	0.75	460
MPP 26u			26	0.75	460
MPP 125u			125	0.75	460
MPP 147u			147	0.75	460
MPP 200u			200	0.75	460

Table 6 Availability of magnetic materials with respect to core shape

	E	ETD	U	Toroid (T_c)
Ferrite	X	X	X	X
Nano-crystalline			X[a]	X
Amorphous			X[a]	X
Powder				X

[a]Materials not considered in this study because they are available with narrow volume range

Table 7 Volume range (mm^3) of magnetic cores for ferrite materials used in the discrete optimization [43–48]

Core	EPCOS ferrite materials		Magnetics ferrite materials	
	Smallest core	Biggest core	Smallest core	Biggest core
EE	33	71,800	78	72,300
EI			1920	11,900
ETD	5350	51,200	5470	51,500
UU	159,000	508,950	350	199,000
UI	116,000	198,000	283	158,000
Toroid	3	172,440	4.3	161,086

References

1. Billings KL (1989) Switchmode power supply handbook. McGraw-Hill, New York
2. Pressmann AI, Billings KL, Morey T (2009) Switchmode power supply design, 3rd edn. McGraw-Hill, New York
3. Maniktala S (2006) Switching power supplies A to Z. Elsevier, Amsterdam
4. Lenk R (2005) Practical design of power supplies. Wiley, New York
5. Brown M (1990) Practical switching power supply design. Academic Press, London
6. Kazimierczuk MK (2008) Pulse-width modulated DC–DC power converters. Wiley, New York
7. McLyman CT (2004) Transformer and inductor design handbook. Marcel Dekker, New York
8. Petkov R (1996) Optimum design of a high-power, high-frequency transformer. IEEE Trans Power Electron 11(1):33–42
9. Hurley WG, Wölfle WH, Breslin JG (1998) Optimized transformer design: inclusive of high-frequency effects. IEEE Trans Power Electron 13(4):651–659
10. Hurley WG, Wolfle WH (2013) Transformers and inductors for power electronics: theory, design and applications. Wiley, New York
11. Bosshard R, Kolar JW (2016) Comparative multi-objective optimization of 50 kW/85 kHz IPT system for public transport. IEEE J Emerg Sel Top Power Electron 4(4):1370–1382

12. Muhlethaler J, Schweizer M, Blattmann R, Kolar JW, Ecklebe A (2013) Optimal design of LCL harmonic filters for three-phase PFC rectifiers. IEEE Trans Power Electron 28(7):3114–3125
13. Garcia-Bediaga A, Villar I, Rujas A, Mir L, Rufer A (2017) Multi-objective optimization of medium-frequency transformers for isolated soft-switching converters using a genetic algorithm. IEEE Trans Power Electron 32:2995–3006
14. Zou S, Lu J, Mallik A, Khaligh A (2018) Modeling and optimization of an integrated transformer for electric vehicle on-board charger applications. IEEE Trans Transp Electrif 4(2):355–363
15. Cassimere BN, Chan RR, Cale J, Cramer AM, Sudhoff SD (2007) Evolutionary design of electromagnetic and electromechanical devices. In: IEEE
16. Cale J, Sudhoff SD, Chan RR (2009) Ferrimagnetic inductor design using population-based design algorithms. IEEE Trans Power Electron 45(2):726–734
17. Sudhoff SD (2014) Power magnetic devices: a multi-objective design approach. Wiley-IEEE Press
18. Shane GM, Sudhoff SD (2013) Design paradigm for permanent–magnet–inductor-based power converters. IEEE Trans Energy Convers 28(4):880–893
19. Hilal A, Cougo B (2016) Optimal inductor design and material selection for high power density inverters used in aircraft applications. In: International conference on electrical systems for aircraft, railway, ship propulsion and road vehicles & international transportation electrification conference (ESARS-ITEC)
20. Burkart RM, Kolar JW (2017) Comparative η–ρ–σ Pareto optimization of Si and SiC multilevel dual-active-bridge topologies with wide input voltage range. IEEE Trans Power Electron 32(7):5258–5270
21. Andersen TM, Krismer F, Kolar JW, Toifl T, Menolfi C, Kull L, Morf T, Kossel M, Brändli M, Francese PA (2017) Modeling and Pareto optimization of on-chip switched capacitor converters. IEEE Trans Power Electron 32(1):363–377
22. Mejbri H, Ammous K, Abid S, Morel H, Ammous A (2014) Bi-objective sizing optimization of power converter using genetic algorithms application to photovoltaic systems. Int J Comput Math Electr Electron Eng 33(1/2):398–422
23. Barg S, Ammous K, Mejbri H, Ammous A (2017) An improved empirical formulation for magnetic core losses estimation under nonsinusoidal induction. IEEE Trans Power Electron 32(3):2146–2154
24. Reinert J, Brockmeyer A, De Doncker RW (2001) Calculation of losses in ferro- and ferrimagnetic materials based on the modified Steinmetz equation. IEEE Trans Ind Appl 37(4):1055–1061
25. Li J, Abdallah T, Sullivan C (2001) Improved calculation of core loss with nonsinusoidal waveforms. In: IEEE industry applications society annual meeting, pp 2203–2210
26. Li J. Abdallah T, Sullivan C (2002) Accurate prediction of ferrite core loss with nonsinusoidal waveforms using only Steinmetz parameters. In: IEEE workshop on computers in power electronics
27. Mühlethaler J, Bielay J, Kolar JW, Ecklebez A (2012) Improved core loss calculation for magnetic components employed in power electronic systems. IEEE Trans Power Electron 27(2):964–973
28. Shen W, Wang F, Boroyevich D, Tipton C (2008) Loss characterization and calculation of nanocrystalline cores for high-frequency magnetics applications. IEEE Trans Power Electron 23(1):475–484
29. Dowell PL (1966) Effects of eddy currents in transformer windings. Proc IEEE 113(8):1387–1394
30. Ferreira JA (1994) Improved analytical modeling of conductive losses in magnetic components. IEEE Trans Power Electron 9(1):127–131
31. Nan X, Sullivan CR (2003) An improved calculation of proximity-effect loss in high-frequency windings of round conductors. In: IEEE
32. Nan X, Sullivan CR (2004) Simplified high-accuracy calculation of eddy-current losses in round-wire windings. In: IEEE power electron specialists conference
33. Erickson RW (2000) Fundamentals of power electronics. Colorado Power Electronics Center University of Colorado, Boulder Updated May 21
34. Maniktala S (2013) Switching power supply design and optimization (chapter 12). McGraw-Hill, New York
35. Microsemi (2013) Forward and flyback core selection using the LX7309 and industry recommendations, Technical Note
36. Texas Instruments, Magnetics design handbook: power transformer design, power.ti.com/seminars
37. Barg S, Alahdal A, Ammous K, Mejbri H, Ammous A (2016) Optimum design approach of high frequency transformer. In: Asia-Pacific international symposium on electromagnetic compatibility (APEMC)
38. Nanakos AC, Tatakis EC, Papanikolaou NP (2012) A weighted-efficiency-oriented design methodology of flyback inverter for ac photovoltaic modules. IEEE Trans Power Electron 27(7):3221–3233
39. Texas Instruments, 120-V AC, 200-W, 90% efficiency, interleaved flyback for battery charging applications reference design. www.ti.com
40. ON Semicondcutor, 200 W, Single Output Power Supply, www.onsemi.com
41. Vartak C, Abramovitz A, Smedley KM (2014) Analysis and design of energy regenerative snubber for transformer isolated converters. IEEE Trans Power Electron 29(11):6030–6040
42. Dimitrakakis GS, Tatakis EC (2009) High-frequency copper losses in magnetic components with layered windings. IEEE Trans Magn 45(8):3187–3199
43. Handbook of chemistry and physics, HCP, 58th edition, p F-163
44. Epcos data book 2013, Ferrite and accessories. www.epcos.com
45. Magnetics, Ferrite cores. www.mag-inc.com
46. Magnetics, Powder cores. www.mag-inc.com
47. Ferroxcube, Product selection guide 2013. www.ferroxcube.com
48. Finmet, EMC components